

MEASUREMENTS WITH POLARIZED HADRONS

T.-A. SHIBATA

Dept. Physics, Tokyo Institute of Technology, Oh-okayama, Meguro-ku, Tokyo, 152-8551, Japan
E-mail: shibata@nucl.phys.titech.ac.jp

Recent progress in physics with polarized hadrons is described with the emphasis on the spin structure of the nucleon. The nucleon spin problem, which was discovered by EMC in 1988, is now being studied in various experiments. Flavor separation of the quark helicity distributions has been made. Recent observations of asymmetries in deeply virtual Compton scattering (DVCS) and exclusive meson productions provide possibilities to access the total angular momentum carried by quarks in the framework of generalized parton distributions. Single spin azimuthal asymmetries observed in semi-inclusive measurements provide a new handle to determine the transverse quark distributions which are basic but have never been measured so far.

1. Introduction

In the SU(6) framework of flavor and spin, the wavefunction of the proton is described with three quarks uud , where the spins of the two quarks are parallel and the third quark spin is anti-parallel, which produces a total spin of $1/2$. A sketch is given in Fig. 1. The expectation value of the u quark polarization is $2/3$ and that of the d quark is $-1/6$. There is no component of the strange quark in the proton in this scheme.

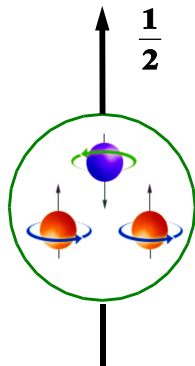


Figure 1. A sketch of the proton where the spins of the three quarks compose the proton spin $1/2$.

This picture was however contradicted by the observation by EMC at CERN in 1988:¹ the quark spin contribution to the proton spin was found to be $(12 \pm 9 \pm 14)\%$ from a deep-inelastic scattering experiment with a longitudinally polarized muon beam on a longitudinally polarized proton target. This is often called the “proton spin problem”. In later experiments on the proton and neutron, the quark spin contribution to the nucleon spin was measured to be 20-30%.

The nucleon is composed of quark spin, gluon spin and orbital angular momenta of quarks and gluons:

$$\frac{1}{2} = \frac{1}{2}\Sigma + \Delta G + L_q + L_g \quad (1)$$

$$\Sigma = \Delta u + \Delta d + \Delta s + \Delta \bar{u} + \Delta \bar{d} + \Delta \bar{s}. \quad (2)$$

Here, Δu for example denotes the helicity difference $u^{\rightarrow}(x) - u^{\leftarrow}(x)$ integrated over the full range of Bjorken x . First of all, the flavor separation of the quark spin contributions to the nucleon spin, namely the separation of $\Delta u, \Delta d, \Delta s, \Delta \bar{u}, \Delta \bar{d},$ and $\Delta \bar{s}$ is important. Deep-inelastic lepton scattering with a good identification capability of produced hadrons is the standard method for it. Combining with the knowledge on the fragmentation functions which describe the quark to hadron formation, one can tag the struck quark in the deep-inelastic scattering process. These measurements are called “semi-inclusive measurements”. The diagram is shown in Fig. 2.

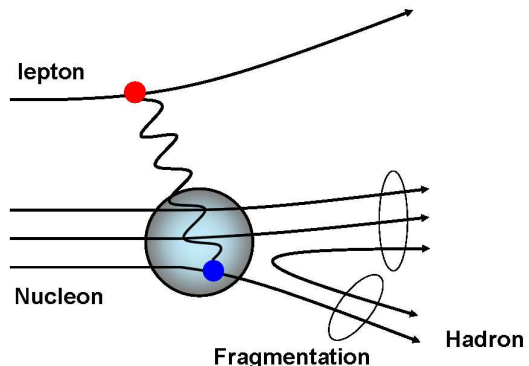


Figure 2. Semi-inclusive measurements of deep-inelastic lepton scattering. A part of produced the hadrons on the bottom are detected in experiments such as HERMES.

The cross sections for inclusive and semi-inclusive measurements are written respectively as

$$\sigma(x) \propto \sum_q e_q^2(x) \quad (3)$$

$$\sigma_h(x, z) \propto \sum_q e_q^2 q(x) D_q^h(z). \quad (4)$$

Here, $q(x)$ is the quark distribution of each flavor, $D_q^h(z)$ the fragmentation function, $h = \pi^\pm, K^\pm, \dots$

The gluon spin contributions are being studied by COMPASS at CERN using muon deep-inelastic scattering. The typical beam energy is 160 GeV. Open charm production from photon-gluon fusion, shown in Fig. 3, are measured.

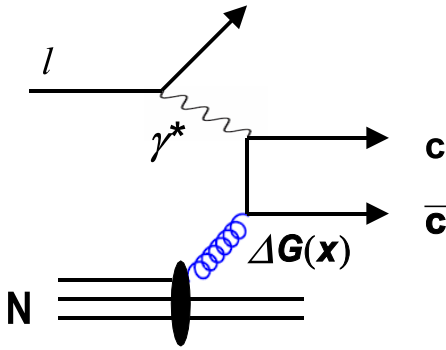


Figure 3. Photon-gluon fusion in deep-inelastic lepton scattering. The virtual photon couples to a quark or to an antiquark from the gluon dissociation.

Another approach to measure the gluon spin contribution is to use polarized proton-proton collisions at RHIC of BNL. Unlike lepton deep-inelastic scattering, major parts of the cross section are determined by strong interactions such as gluon-gluon, gluon-quark and quark-quark collisions. The details are shown in a later section.

2. Flavor Separation of Quark Helicity Distributions

Cross sections for deep-inelastic scattering are cross sections for absorption of a virtual photon.

A quark in the nucleon absorbs the photon by flipping its own spin direction. The left side in Fig. 4 is before the photon absorption, the right side after the photon absorption. The cross section is different for different spin states. The double spin asymmetry

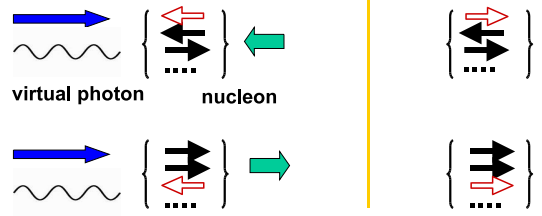


Figure 4. Absorption of a virtual photon by a quark in the longitudinally polarized nucleon.

A_1 arises from this cross section difference. A_1 is related to the cross section:

$$A_1(x) = \frac{\sigma_{\rightarrow\rightarrow}(x) - \sigma_{\rightarrow\leftarrow}(x)}{\sigma_{\rightarrow\rightarrow}(x) + \sigma_{\rightarrow\leftarrow}(x)}. \quad (5)$$

The semi-inclusive asymmetry $A_1^h(x, z)$ can be written as

$$A_1^h(x, z) = \frac{\sum_q e_q^2 \Delta q(x) D_q^h(z)}{\sum_q e_q^2 q(x) D_q^h(z)}. \quad (6)$$

Measurements of A_1 from semi-inclusive π^\pm and K^\pm measurements with a deuterium target at HERMES² are shown in Fig. 5. HERMES uses 27.6 GeV positron or electron beams at DESY-HERA. The data from SMC³ with positive and negative hadron measurements are shown for comparison. The major parts of hadrons are pions. The data with the proton target⁴ was also used in the analysis. A ring imaging Čerenkov detector plays an essential role in the particle identification of hadrons at HERMES.

The inclusive asymmetry increases with Bjorken x . The semi-inclusive asymmetries shown here also increase with Bjorken x reflecting the inclusive cross section. However, the K^- is made of sea quark only ($\bar{u}s$) and the asymmetry is consistent with zero.

The quark helicity distributions are extracted from the observed asymmetries: $A(x) = P(x)Q(x)$. $A(x) = (A_{1p}, A_{1p}^{\pi^+}, A_{1p}^{\pi^-}, A_{1d}, A_{1d}^{\pi^+}, A_{1d}^{\pi^-}, A_{1d}^{K^+}, A_{1d}^{K^-})$ is the asymmetry in inclusive and semi-inclusive measurements with the proton and deuterium targets while $Q(x) = (\frac{\Delta u}{u}, \frac{\Delta d}{d}, \frac{\Delta \bar{u}}{\bar{u}}, \frac{\Delta \bar{d}}{d}, \frac{\Delta s}{s})$ is the quantity to be extracted. $\frac{\Delta \bar{s}(x)}{\bar{s}(x)}$ was allowed to move from minimum to maximum in the present analysis and its effect on the other five parameters were included in the systematic errors. $P(x)$ is a matrix. The matrix elements contain information on the fragmen-

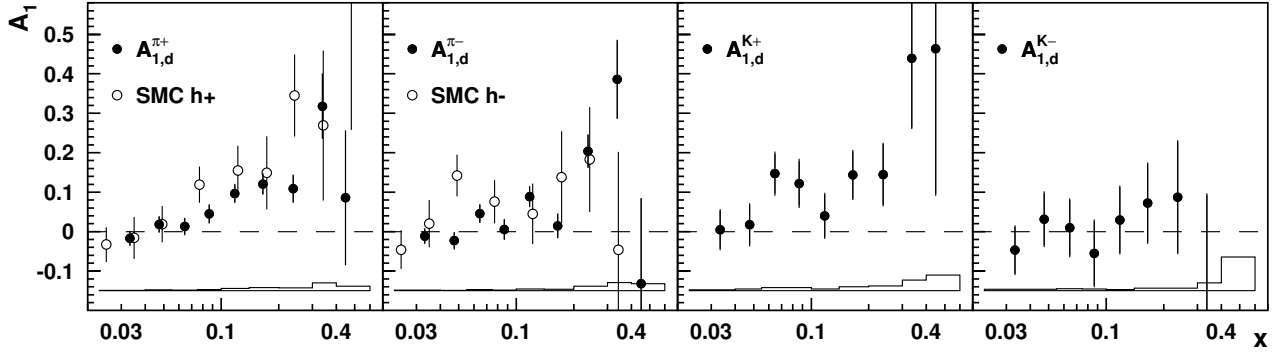


Figure 5. Double spin asymmetry A_1^h of semi-inclusive deep-inelastic scattering at HERMES with the deuterium target. The data of SMC for positive and negative hadrons are also shown for comparison.

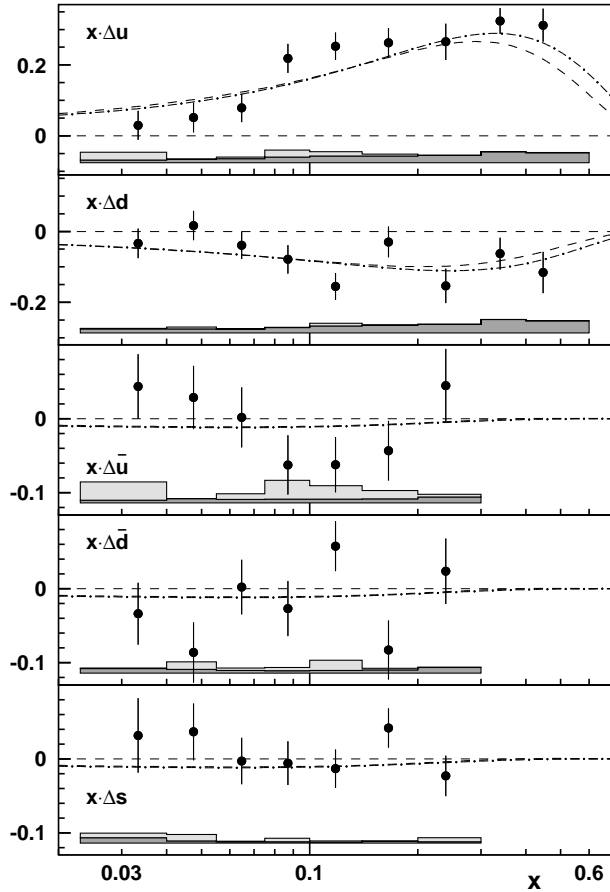


Figure 6. Flavor separation of the quark helicity distributions by HERMES.

tation. The elements are evaluated with a Monte Carlo which was tuned to approximate the hadron multiplicities measured at HERMES.

The results are shown in Fig. 6. The bands show systematic errors. The curves show QCD fits to inclusive measurements.⁵ The helicity distribution of the u quark is positive while that of the d quark is negative. The helicity distributions of sea quarks are close to zero.

It should be noted that the flavor separation is done in each x bin independently except for small corrections for smearing due to the finite kinematical resolution of the spectrometer. It is not necessary to assume any functional forms in the measured and unmeasured regions of x . It is also not necessary to prefix the first moment of the quark helicity distribution, namely integration over Bjorken x , using information from other experiments such as neutron beta-decay and hyperon weak decays.

The measurements of the inclusive asymmetry A_1 with proton and neutron targets at large Bjorken x at JLab enables the flavor separation at large x since the sea quark contributions are small there.

3. Deeply Virtual Compton Scattering and Generalized Parton Distributions

The cross section for deep-inelastic scattering is given by the total absorption cross section of a virtual photon as mentioned before. It is therefore equivalent to the imaginary part of the forward elastic amplitude. “Elastic” in this case means Compton scattering.

Deeply virtual Compton scattering (DVCS) is similar, but is different in a sense that a real photon

is produced in the final state as shown in Fig. 7. A momentum fraction has to be taken out and put back as shown in Fig. 7. Therefore, the amplitude involved is not the forward one but is off-forward.

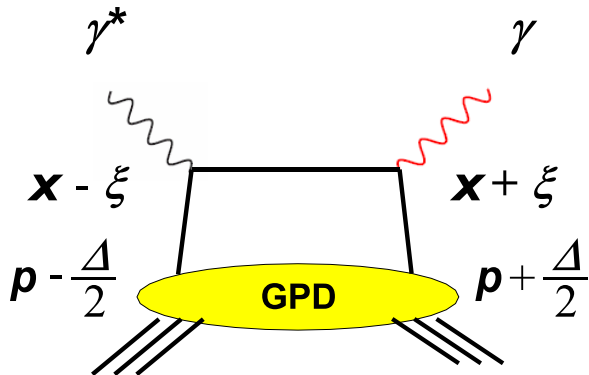


Figure 7. Diagram of deeply virtual Compton scattering (DVCS).

Recently DVCS received attention as it plays an important role in determining the generalized (sometimes called the off-forward or skewed) parton distributions. In the framework of the generalized parton distributions various observables such as DVCS, elastic form factors, quark distributions from deep-inelastic scattering etc. are coherently analyzed as shown in Fig. 8. There are four generalized parton distributions concerning quarks: $H^q(x, \xi, t)$, $E^q(x, \xi, t)$, $\tilde{H}^q(x, \xi, t)$, and $\tilde{E}^q(x, \xi, t)$. In the forward limit where $t \rightarrow 0$ and $\xi \rightarrow 0$, $H^q(x, 0, 0)$ and $\tilde{H}^q(x, 0, 0)$ are reduced to $q(x)$ and $\Delta q(x)$, the ordinary quark distributions and helicity distributions, respectively. When integrated over x and summed over q , $H^q(x, \xi, t)$ and $E^q(x, \xi, t)$ are reduced to $F_1(t)$ and $F_2(t)$, the Dirac and Pauli nucleon form factors, respectively, while $\tilde{H}^q(x, \xi, t)$ and $\tilde{E}^q(x, \xi, t)$ are reduced to $g_A(t)$ and $h_A(t)$, the axial-vector and pseudo-scalar form factors, respectively.

Once the generalized parton distributions are determined, the total angular momentum contribution of the quarks J_q to the nucleon spin can be evaluated:⁶

$$\lim_{t \rightarrow 0} \frac{1}{2} \int_{-1}^{+1} dx x [H^q(x, \xi, t) + E^q(x, \xi, t)] = J_q. \quad (7)$$

Since the quark spin contribution $\frac{1}{2}\Sigma$ is already known, one can then determine the contributions of the orbital angular momentum of the quarks L_q to the nucleon spin: $J_q = L_q + \frac{1}{2}\Sigma$. So far not many theoretical methods to access the orbital angular momen-

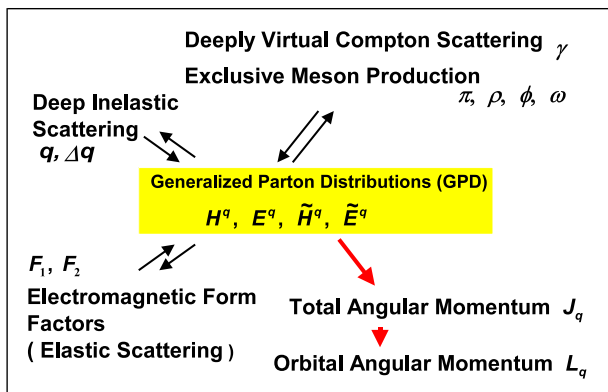


Figure 8. Relations of generalized parton distributions.

tum of quarks have been proposed, and the method mentioned above is an attractive one.

The processes to produce a direct photon are the DVCS and Bethe-Heitler processes. The latter involve the production of a photon from the initial or final lepton line. The cross section for direct photon production is therefore expressed as

$$\frac{d^4\sigma}{d\phi dt dQ^2 dx} \propto |A_{DVCS} + A_{BH}|^2 \quad (8)$$

$$= |A_{DVCS}|^2 + |A_{BH}|^2 + I \quad (9)$$

where I is the interference term between the DVCS and Bethe-Heitler amplitudes.

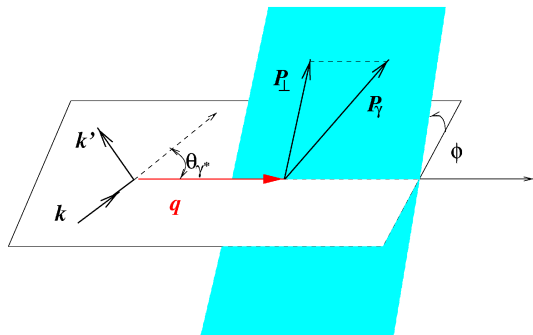


Figure 9. Definition of azimuthal angle ϕ .

The single spin asymmetry from a polarized positron beam with an unpolarized nucleon target is

$$\Delta\sigma_{LU} = \sigma(e^+p) - \sigma(e^-p) \propto -\sin\phi \times \text{Im} I. \quad (10)$$

The beam charge asymmetry from positron and electron beams is

$$\Delta\sigma_{ch} = \sigma(e^+p) - \sigma(e^-p) \propto \cos\phi \times \text{Re} I. \quad (11)$$

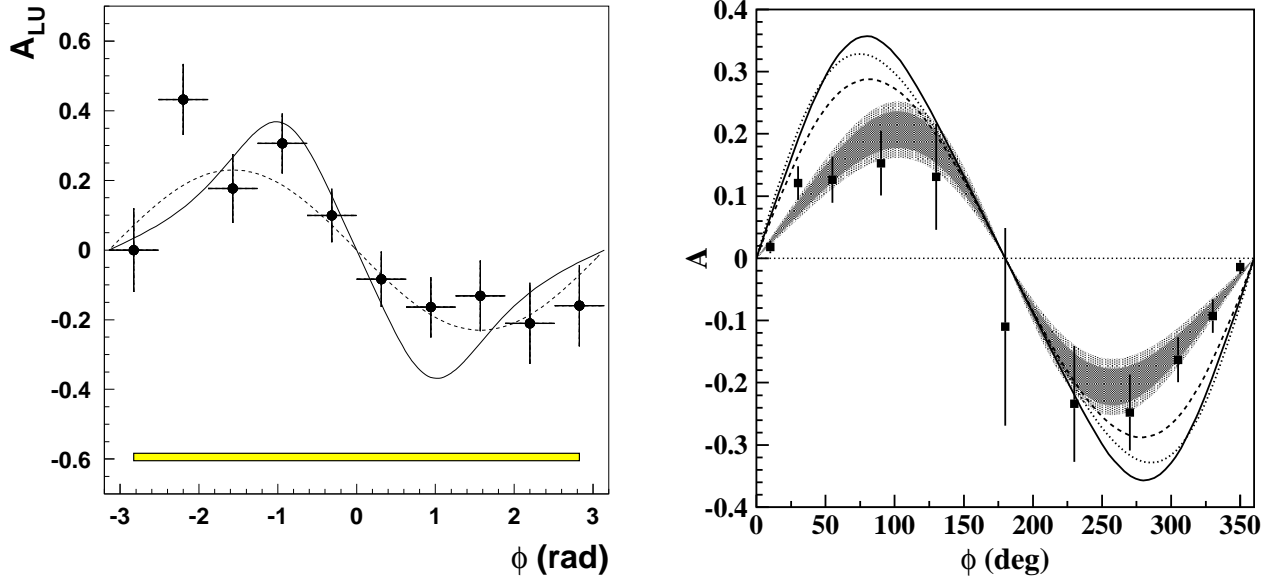


Figure 10. Beam spin asymmetry due to the interference between DVCS and Bethe-Heitler processes observed by HERMES (left) and CLAS (right)

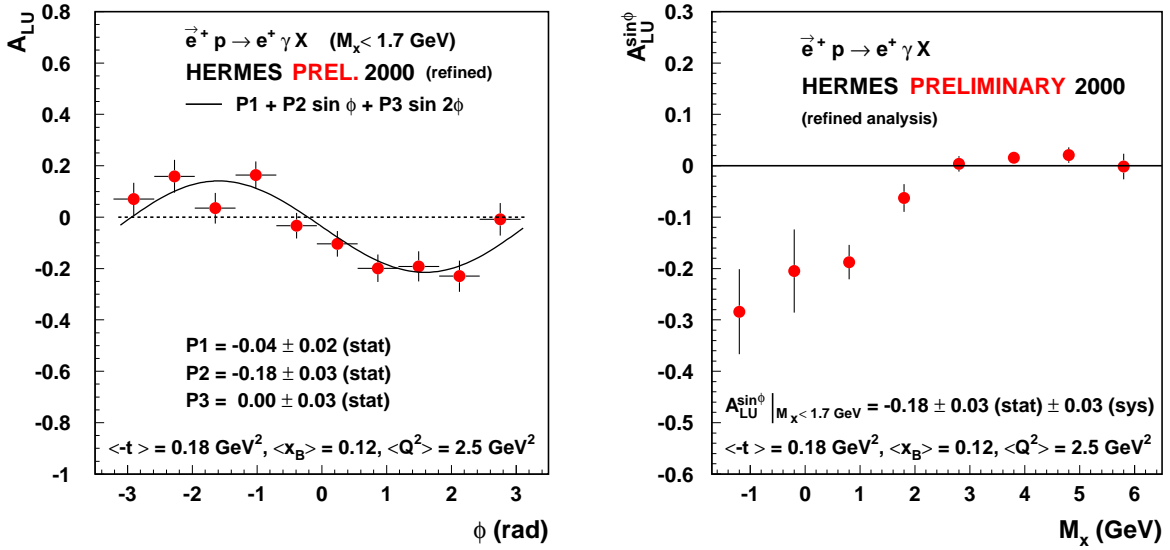


Figure 11. Beam spin asymmetry (left) and the $\sin \phi$ moment (right) of DVCS as a function of the missing mass.

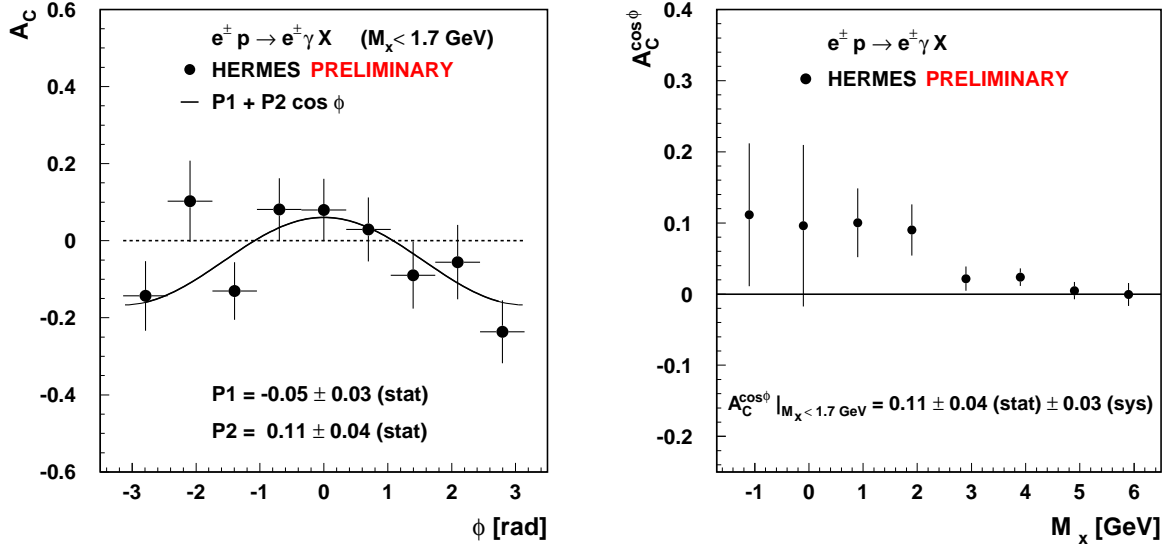


Figure 12. Beam charge asymmetry (left) and the $\cos\phi$ moment (right) of DVCS as a function of the missing mass.

The angle ϕ is the azimuthal angle defined in Fig. 9. The σ_{LU} was measured by HERMES⁷ and CLAS.⁸ The quantity σ_{ch} was measured by HERMES as both positron and electron beams are available at DESY. This way one can access the imaginary and real parts of the interference term. At higher energies the direct photon production is dominated by DVCS, so the DVCS cross section, not asymmetry, is measured by H1 and ZEUS.

The single spin asymmetries, A_{LU} , observed by HERMES and CLAS are shown in Fig. 10. The single spin asymmetry, A_{LU} , with updated statistics from HERMES and the missing mass distribution of its $\sin\phi$ moment are shown in Fig. 11. The beam charge asymmetry, A_c , from HERMES and the missing mass distribution of its $\cos\phi$ moment are shown in Fig. 12. The missing mass resolution is 0.8 GeV. In the region of the missing mass which corresponds to the nucleon mass, significant deviations of the moments from zero are observed.

To further extend the studies of the generalized parton distributions, exclusive meson productions⁹ are useful. In these cases a meson is produced instead of a photon. When a pseudoscalar meson such as a π is produced, \tilde{H}^q and \tilde{E}^q are sensitive to these processes. When a vector meson such as a ρ , ϕ , or ω is produced, H^q and E^q are probed.

4. Quark Transversity Distributions

There are three leading twist (twist-two) quark distributions: ordinary quark distribution $q(x)$, helicity distribution $\Delta q(x)$, and transversity distribution $\delta q(x)$. A sketch is given in Fig. 13.

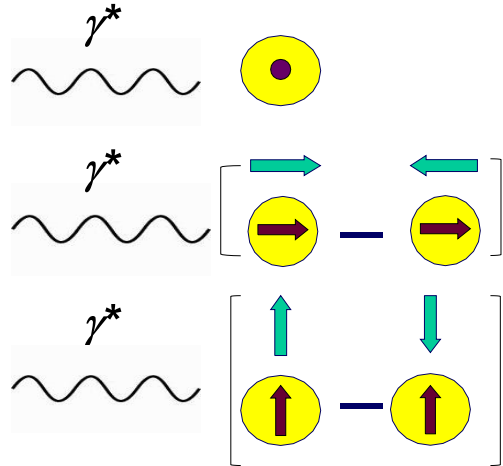


Figure 13. Three types of quark distributions: unpolarized distribution $q(x)$, helicity distribution $\Delta q(x)$, and transversity distribution $\delta q(x)$.

The spin averaged distribution is denoted by $q(x)$. It indicates a vector charge when integrated over x . $\Delta q(x)$ is the helicity difference. It represents the axial charge when integrated over x . $\delta q(x)$ is the

helicity flip type, and represents the tensor charge. $\delta q(x)$ is chiral odd, so it is not accessed in inclusive deep-inelastic scattering. However, it is accessible with semi-inclusive measurements of deep inelastic scattering because $\delta q(x)$ can be accompanied with another chiral odd object, namely a chiral odd fragmentation function:

$$A_1^h \approx \sum_q e_q^2 \delta q(x) \cdot H(z)_{1,q}^{\perp h}. \quad (12)$$

The quantity $q(x)$ has been very well measured, and $\Delta q(x)$ has been well measured, too. $\delta q(x)$ is the last unmeasured twist-two distribution, which attracted theoretical attention recently in parallel with the realization of the experimental feasibility in deep-inelastic scattering.

The three distributions are not independent. They are related by a Soffer bound:

$$|\delta q(x)| \leq \frac{1}{2} |q(x) + \Delta q(x)|. \quad (13)$$

Since $\delta q(x)$ does not couple with the gluon, the Q^2 evolution should be different from that of $q(x)$ and $\Delta q(x)$. This is another interesting point.

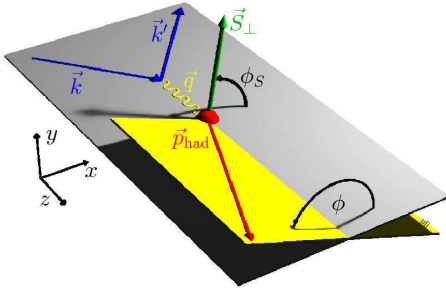


Figure 14. Definition of ϕ_s angle in the case of a transversely polarized target.

The data for which analyses were completed by HERMES are those using longitudinally polarized targets. The virtual photon emitted in each event from the incoming positron beam has a certain transverse component with respect to the positron beam axis. Therefore, the effect of transversity could show up already with the longitudinally polarized targets:

$$A_{UL}^{sin\phi} \sim S_L \langle \sin\phi \rangle_{UL} - S_T \langle \sin\phi \rangle_{UT}. \quad (14)$$

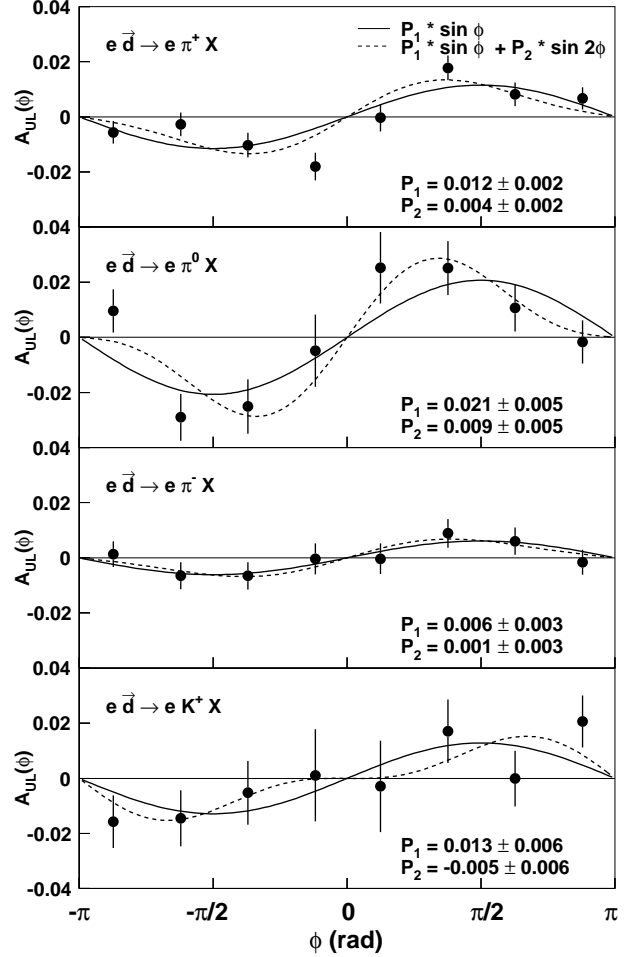


Figure 15. Single spin azimuthal asymmetries A_{UL} in semi-inclusive measurements of deep inelastic scattering

The transverse component of the virtual photon, S_T , is expressed as

$$S_T \approx \frac{2Mx}{Q} \sqrt{1-y} \quad (15)$$

$$\leq \sin\theta_\gamma \gtrsim 0.15. \quad (16)$$

With the data being taken by HERMES since 2002 with a transversely polarized proton target, analyses can be further developed since there is an angle ϕ_s in addition to ϕ as shown in Fig. 14. The Collins effect is expected to show a $\sin(\phi + \phi_s)$ moment while the Sivers effect is expected to show a $\sin(\phi - \phi_s)$ moment. HERMES has already accumulated 700K events and COMPASS has also taken data. From the data taken so far using the longitudinally polarized target, the azimuthal angle dependence of the asymmetry A_{UL} was measured. The

results on the proton target¹⁰ and on the deuterium target¹¹, shown in Fig. 15, were obtained. In Fig. 15 the $\sin\phi$ moment is positive for π^+ , π^0 and K^+ . It increases with Bjorken x , suggesting that the valence quark or u quark plays the dominant role. The $\sin\phi$ moment is small for π^- .

With the new results from the transversely polarized target, it is expected that the physics of quark transversity distributions will be developed extensively.

JLab has also an experimental program to study this subject.

5. Polarized Proton-Proton Collisions

One of the aims of using polarized proton-proton collisions at RHIC of BNL is to study the gluon spin contribution to the proton spin. A longitudinally polarized proton beam is required to measure the helicity distributions of the partons in the proton. The physics goal or milestone is to achieve a beam polarization of 70% and an integrated luminosity of 320 pb⁻¹ at $\sqrt{s} = 200$ GeV and 800 pb⁻¹ at $\sqrt{s} = 500$ GeV. A beam polarization of about 30% and an integrated luminosity of about 0.4 pb⁻¹ were achieved in 2003. The goals are expected to be reached several years from now.

The PHENIX collaboration plans to measure the gluon helicity distribution $\Delta G(x)$ from the asymmetry A_{LL} in direct photon production from quark-gluon collisions. The process is shown in Fig. 16 and is called ‘‘gluon Compton scattering’’. In the p_T region below 10 GeV the quark-gluon collision is dominant over gluon-gluon and quark-quark collisions. The STAR collaboration plans to measure the asymmetry in di-jet productions which also has a significant dependence on the gluon polarization in the proton.

The single spin asymmetry A_N in π^0 production at forward angles from transversely polarized proton collisions, $p^\uparrow + p \rightarrow \pi^0 + X$, has been measured by STAR as shown in Fig. 17. The asymmetry resembles the results from the earlier fixed target experiment E704 at Fermilab, in spite of the fact that \sqrt{s} is now 200 GeV compared to 20 GeV at E704. The p_T is low also in the present measurement. Here again, the contributions of the Collins effect and the Sivers effect, as well as higher-twist contributions are being investigated.

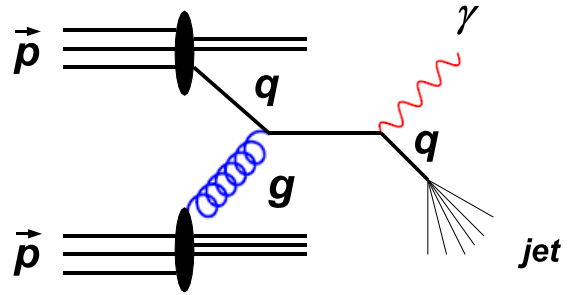


Figure 16. Diagram of $pp \rightarrow \gamma + X$. This process is called gluon Compton scattering.

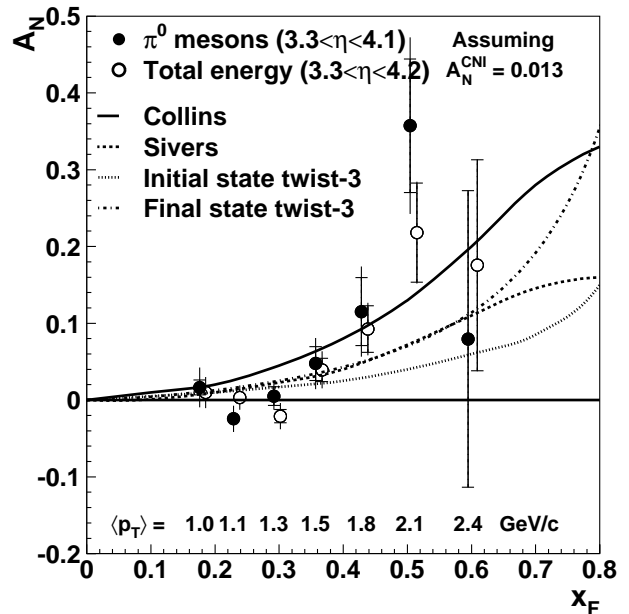


Figure 17. Single transverse beam spin asymmetry A_N in π^0 production at forward angles measured by STAR.

The asymmetry A_{LL} in π^0 production in the central rapidity region from longitudinally polarized proton collisions is being analysed by PHENIX.

6. Summary

To understand hadrons in terms of QCD, the spin structure of the nucleon is an important subject. Many experiments are currently running with e , μ , γ , p ... beams. Flavor separation of the quark helicity distributions, $\Delta q(x)$, have been made using semi-inclusive measurements of produced hadrons in deep-inelastic lepton scattering. Asymmetries in DVCS and in exclusive meson production provide access to generalized parton distributions. It is expected that

contributions of the orbital angular momentum of quarks to the nucleon spin can be evaluated in the framework of generalized parton distributions.

Single-spin azimuthal asymmetries have been observed in semi-inclusive measurements of deep-inelastic scattering. Quark transversity distributions, $\delta q(x)$, are basic in the sense that they are twist-two distributions but have never been determined so far. Results from transversely polarized targets will become available soon.

The polarized proton-proton collider now has longitudinally as well as transversely polarized beams. The single spin asymmetry A_N in π^0 productions at small angles from a transversely polarized beam have been obtained. The asymmetries at large p_T are being analyzed.

Spin physics with hadrons is a rapidly expanding field: many new ideas for measurements have been proposed and high precision data are being accumulated. We might have new surprises from these studies.

Acknowledgments

The author wishes to thank all the colleagues who made the large progress in spin physics in recent years possible.

References

1. J. Ashman *et al.*, *Phys. Lett. B* **206**, 364 (1988);
J. Ashman *et al.* *Nucl. Phys. B* **328**, 1 (1989).
2. A. Airapetian *et al.*, hep-ex **0307064**, (2002).
3. B. Adeva *et al.*, *Phys. Lett. B* **420**, 180 (1998).
4. K. Ackerstaff *et al.*, *Phys. Lett. B* **464**, 123 (1999).
5. M. Glueck *et al.*, *Phys. Rev. D* **63**, 094005 (2001);
J. Bluemlein and H. Boettcher, *Nucl. Phys. B* **636**, 225 (2002).
6. X. Ji, *Phys. Rev. Lett.* **78**, 610 (1997).
7. A. Airapetian *et al.*, *Phys. Rev. Lett.* **87**, 182001 (2001).
8. S. Stepanyan *et al.*, *Phys. Rev. Lett.* **87**, 182002 (2001).
9. A. Airapetian *et al.*, *Phys. Lett. B* **535**, 85 (2002).
10. A. Airapetian *et al.*, *Phys. Rev. Lett.* **84**, 4047 (2000);
A. Airapetian *et al.*, *Phys. Rev. D* **64**, 097101 (2001).
11. A. Airapetian *et al.*, *Phys. Lett. B* **562**, 182 (2003).
12. A. Airapetian *et al.*, *Phys. Rev. D* **64**, 112005 (2001).

DISCUSSION

Ikaros Bigi (Notre Dame): Are there any recent data on the question of how the longitudinal polarization of the incoming lepton beam, either muon or neutrinos, are transferred into the final state by looking at polarizations of Λ , Ξ and even charm baryons?

Toshi-Aki Shibata: New data are being analyzed for longitudinal Λ polarization by HERMES in addition to the already published results.¹² COMPASS could also contribute to this subject.